

## MICROPATTERNED HYDROGENATED AMORPHOUS CARBON GUIDES MESENCHYMAL STEM CELLS TOWARDS NEURONAL DIFFERENTIATION

F. D'Angelo<sup>1§</sup>, I. Armentano<sup>2§</sup>, S. Mattioli<sup>2</sup>, L. Crispoltoni<sup>1</sup>, R. Tiribuzi<sup>1</sup>, G.G. Cerulli<sup>3</sup>, C.A. Palmerini<sup>4</sup>,  
J.M. Kenny<sup>5\*\*</sup>, S. Martino<sup>1\*</sup>, and A. Orlacchio<sup>1\*</sup>

<sup>1</sup> Department of Experimental Medicine and Biochemical Sciences, Section of Biochemistry and Molecular Biology, University of Perugia, Italy

<sup>2</sup> Materials Engineering Centre, UdR INSTM, NIPLAB, University of Perugia, Terni, Italy;

<sup>3</sup> Department of Orthopedics and Traumatology, University of Perugia, Perugia, Italy;

<sup>4</sup> Department of Internal Medicine, laboratory of Biochemistry, University of Perugia, Perugia, Italy;

<sup>5</sup> Materials Engineering Centre, University of Perugia, UdR INBB, Terni, Italy;

\*\* current address: ICTP-CSIC, Madrid, Spain.

§ F. D'Angelo and I. Armentano contributed equally to this study.

### Abstract

This study investigated how the design of surface topography may stimulate stem cell differentiation towards a neural lineage. To this end, hydrogenated amorphous carbon (a-C:H) groove topographies with width/spacing ridges ranging from 80/40µm, 40/30µm and 30/20µm and depth of 24 nm were used as a single mechanotransducer stimulus to generate neural cells from human bone marrow mesenchymal stem cells (hBM-MSCs) *in vitro*. As comparative experiments, soluble brain-derived neurotrophic factor (BDNF) was used as additional biochemical inducer agent. Despite simultaneous presence of a-C:H micropatterned nanoridges and soluble BDNF resulted in the highest percentage of neuronal-like differentiated cells our findings demonstrate that the surface topography with micropatterned nanoridge width/spacing of 40/30µm (single stimulus) induced hBM-MSCs to acquire neuronal characteristics in the absence of differentiating agents. On the other hand, the alternative a-C:H ridge dimensions tested failed to induce stem cell differentiation towards neuronal properties, thereby suggesting the occurrence of a mechanotransducer effect exerted by optimal nano/microstructure dimensions on the hBM-MSCs responses.

**Keywords:** Biological response, cell/protein-material interactions, biomaterial surfaces, tissue engineering, regenerative medicine, cytoskeleton, stem cell differentiation.

### Introduction

Interfaces between engineered materials and stem cells play a critical role in biomedical applications where the interaction between cells and material surface dictates cell performance and the success of an implanted device. Cells can act as mechanosensitive units responding to the mechanical stimulation of the extracellular matrix through focal adhesions and changes in cytoskeletal organization (Curtis and Varde, 1964; Curtis, 2004; Engler *et al.*, 2006; Dalby *et al.*, 2007a; Dalby, 2009; Biggs *et al.*, 2010). Mechanotransduction may involve changes in the positioning of ion channels, G-proteins and kinases (Burridge *et al.*, 1996) through, for example, stretch (Eastwood *et al.*, 1998) or contact guidance (Clark *et al.*, 1991). This leads to the induction of signaling cascades affecting cellular behavior, for example, proliferation or differentiation (Biggs *et al.*, 2009). Alternatively, mechanotransduction may also be due to changes in tension through the cytoskeleton (Ingber, 1993; Charras and Horton, 2002; Dalby, 2005). For instance, a nanoscale topography disorder was shown to stimulate human mesenchymal stem cells to produce bone mineral in the absence of osteogenic supplements *in vitro* (Dalby *et al.*, 2007b), whereas the combination of regulatory molecules and the cell location inside the materials influenced the cell differentiation process toward osteogenic or adipogenic lineages (Ruiz and Chen, 2008). Furthermore, Chen and collaborators showed that ultra-nanocrystalline-diamond employed as the culture substrate exerted the differentiation of neural stem cells in the absence of differentiating agents (Chen *et al.*, 2010).

Recently, we have explored the interface between human bone marrow mesenchymal stem cells (hBM-MSCs) and hydrogenated amorphous carbon (a-C:H) film designed with uniform, groove or grid nanostructures. We demonstrated that hBM-MSCs responded to different pattern designs with specific changes of microtubule organization. In particular, we observed that the grid pattern induced a square-localized distribution of  $\beta$ -tubulin/actin fibres, while the ridge pattern exerted a more dynamic effect, associated with microtubule alignment and elongation (Martino *et al.*, 2009a).

In this study, we posed the question whether the interaction between hBM-MSCs and a-C:H with micropatterned nanoridges could be useful for neural

\*Address for correspondence:

Prof. Aldo Orlacchio

Via del Giochetto

06126 Perugia, Italy

Telephone/FAX Number: +390755852187,

E-mail: orly@unipg.it; martin@s@unipg.it.

differentiation. We designed a study where hBM-MSCs, the adult stem cells able to differentiate towards osteoblasts, adipocytes, muscle and neural cells (Orlacchio *et al.*, 2010a; Orlacchio *et al.*, 2010b; Martino *et al.*, 2009b; Prockop, 1997; Sanchez-Ramos, 2002; Stewart and Przyborski, 2002; Grove *et al.*, 2004), were seeded on a-C:H nanofilms with ridge microtopographies (defined as 200P, 300P, 400P) in the presence/absence of soluble brain-derived neurotrophic factor (BDNF).

In the present report, we demonstrate that the maximal production of neuronal-like cells from hBM-MSCs *in vitro* was obtained through a combination of topography (physical stimulus) and BDNF (chemical stimulus). Notably, we found that large populations of neuronal-derived stem cells were also obtained without BDNF treatment by simply employing surface topography featuring ridges with width/spacing of 40/30  $\mu\text{m}$ .

## Materials and Methods

### a-C:H micropatterned nanoridges preparation and characterization

The a-C:H nanopatterned films were prepared by means of a radiofrequency plasma-enhanced chemical vapour deposition (rf-PECVD) method using a Sistec apparatus with a Huttinger power supply at 13.56 MHz. Glass cover slips (13mm diameter) cleaned with ethanol were used as substrates, three different masks named 200P, 300P and 400P (with nominal microstructure of 200, 300 and 400 ridges/inch) were used to develop the specific nanoridges. The cleaned cover slips were placed in the chamber, with a mask on the top layer, to obtain the desired nanotopography. The stainless steel chamber was evacuated for 1 h to achieve a pressure (P) of  $10^{-2}$  Torr, and the deposition was performed using methane gas at 32 sccm flow rate. The deposition conditions were as follows: P =  $8 \times 10^{-2}$  Torr; power supply (RF) = 15-30 W; bias voltage (V) = 240-340 V; and time = 5-20 min.

Micropatterned morphology was investigated using a field emission scanning electron microscope (FESEM, Supra 25 Zeiss, Welwyn Garden City, UK), operating at an accelerating voltage of 1 kV. The topography of the nanopatterned films was analyzed by atomic force microscopy (easy Scan AFM, Nanosurf, Liestal, Switzerland). AFM images were recorded in tapping mode at room temperature in air, using silicon cantilevers and a scan rate of 0.3s/line.

The thickness of a uniform layer of a-C:H was determined with a spectroscopic ellipsometer (M-2000, J.A. Woollam Co., Lincoln, NE, USA). The thickness and the optical constant were measured across a wavelength spectrum ranging between 245 and 1000 nm. Measurements were performed at two incident angles:  $50^\circ$  and  $60^\circ$ . The models used for the determination of optical constants were Tauc-Lorentz and Lorentz, considering that optical absorption of the deposited films was detectable throughout almost the entire range of measurements.

Optical absorption measurements were performed on every film configurations using a Perkin-Elmer (Waltham,

MA, USA) UV-VIS-NIR spectrometer (Lambda-35) set to scan from 250 to 1100 nm at room temperature; the spectra obtained by modulating the power supply and treatment time were compared and the film thickness measured using the Lambert-Beer law ( $A = \alpha \cdot t$ ).

Static contact angle measurements were used to investigate the wettability and the surface energy of the amorphous and patterned carbon thin films. The determination of surface energy was based on the Owens and Went (1969) method and two test liquids (distilled water and diiodomethane) were used as a probe for calculations. The contact angles were assessed using the sessile drop method in air using a FTA1000 Analyzer (Dinwiddie Street, Portsmouth, VA, USA). Drops of either sterile water (high-performance liquid chromatography grade water) and diiodomethane with a volume of 20  $\mu\text{L}$  were placed on films, and measurements were recorded 10 sec after the liquid made contact with the surface. Five independent measurements at different sites were averaged.

### hBM-MSCs isolation and culture

hBM-MSCs were isolated and cultured as previously described (Martino *et al.*, 2009a). Briefly, bone marrow cells were taken from the medullary cavities of the femurs of patients undergoing primary total hip replacement. Informed consent was obtained from all donors, and the institutional ethical committee approved the procedures. Bone marrow was diluted with phosphate buffered saline (PBS) without  $\text{Ca}^{2+}$  and  $\text{Mg}^{2+}$  supplemented with 2mM ethylenediaminetetra-acetic acid, and mononuclear cells were isolated by density gradient on Lympholyte (Cedarlane Laboratories, www.cedarlanelabs.com). Human bone mononuclear cells were seeded in 25  $\text{cm}^2$  tissue-culture flasks at a density of  $2.5 \times 10^6$  cells/mL and grown in RPMI-1640 (Euroclone, Sizzano (PV) Italy) containing 10% heat-inactivated fetal bovine serum (FBS), 2mM of L-glutamine, and 100U/mL of penicillin-streptomycin (Euroclone). Tissue cultures were incubated at  $37^\circ\text{C}$  in a humidified atmosphere with 5% carbon dioxide ( $\text{CO}_2$ ). After a 5-7 day culture, non-adherent cells were discarded, and fresh medium added. After 15 days, fibroblast-like colonies became visible. The medium was changed every 3 days. hBM-MSCs were used for differentiation experiments.

### Differentiation of hBM-MSCs toward neural cells

hBM-MSCs were plated on tissue culture polystyrene chamber slides at a density of  $2 \times 10^3$  cells  $\times$   $\text{cm}^2$ . During the first 24 h, cells were cultured in control medium (RPMI 1640, 10% FBS, 100U/mL of penicillin-streptomycin, 2mM of L-glutamine). Neural differentiation was achieved using neural medium (RPMI 1640, 100U/mL of penicillin-streptomycin, 2mM of L-glutamine), supplemented with 50ng BDNF (Sigma-Aldrich), 135ng  $\beta$ -FGF (Sigma-Aldrich), and 10ng PDGF-AA (Sigma-Aldrich). Undifferentiated cultures were maintained in control medium without FBS (RPMI 1640, 100U/mL of penicillin-streptomycin, 2mM of L-glutamine). All cell substrates were maintained for 12 days in a humidified incubator at  $37^\circ\text{C}$  and 5%  $\text{CO}_2$ , with medium changes every 3 days

(Prockop, 1997; Sanchez-Ramos, 2002; Stewart and Przyborski, 2002; Grove *et al.*, 2004; Dezawa *et al.*, 2004; Magaki *et al.*, 2005).

### BDNF treatment of hBM-MSCs cultured on a-C:H nanopatterns

hBM-MSCs were plated on a-C:H patterned substrates (200P, 300P and 400P), glass cover slips, a-C:H film and tissue culture polystyrene (TCP) at a density of  $2 \times 10^3$  cells  $\times$  cm<sup>2</sup> in normal growth medium (RPMI 1640, 10%FBS, 100U/mL of penicillin-streptomycin, 2mM of L-glutamine) during the first 24 h. After this time, normal growth medium was removed and replaced with RPMI 1640 supplemented with soluble BDNF (50ng BDNF from Sigma-Aldrich) and 100U/mL of penicillin-streptomycin, 2mM of L-glutamine. Undifferentiated cultures were maintained in control medium (RPMI 1640, 100U/mL of penicillin-streptomycin, 2mM of L-glutamine). Cultures were carried out in a humidified incubator at 37°C and 5% CO<sub>2</sub>, with medium changes every 3 days.

### Cell viability assay

To establish cell viability, hBM-MSCs were plated on different substrates (glass cover slip, TCP, a-C:H film, and micropatterned nanoridges) at a starting concentration of  $2 \times 10^3$  cells/mL in control medium. At different time points (3, 7 and 12 days), cell viability was measured by assaying mitochondrial dehydrogenase activity using the XTT salt solution kit (Sigma-Aldrich). The absorbance of the samples was measured on a microtiter plate reader (GDV) at 450 nm (reference 650 nm).

### Electrochemical assay detection of NO metabolites

Liberated nitric oxide (NO) was measured by chemical reduction using an electrochemical apparatus consisting of a reaction vessel (5mL) subjected to a 5ml/min N<sub>2</sub> flow at a constant temperature (25°C) (Palmerini *et al.*, 1998; Palmerini *et al.*, 2000; Palmerini *et al.*, 2003). The NO formed in the vessel was carried by N<sub>2</sub> current to an amperometric sensor. Aliquots of the samples (20-50μL) were transferred to the reaction vessel containing 2mL of 0.1M CuCl<sub>2</sub> + 0.1M cysteine. The apparatus was calibrated by injecting known amounts of standard nitrite solution into the reaction vessel containing CuCl and cysteine. The height of current peaks was linearly released according to the amount of added nitrite (correlation coefficient  $\geq 0.98$ ). The lowest detectable amount of NO was 10-20nM (corresponding to 10-20pmol in the reaction vessel). Linearity was observed up to 100mM.

### Immunofluorescence

Immunofluorescence to assess neural differentiation was performed after 12 days of culture. Cells were rinsed twice with PBS, fixed in 4% paraformaldehyde for 30 min and, after additional PBS washing, permeabilized blocked (PBS+10% FBS, 0.1% Triton X-100) for 1h at RT, incubated for 20 min with AlexaFluor 488 phalloidin to stain F-actin, and finally subjected to immunostaining. Primary antibodies, were anti-β-Tubulin, anti-vinculin, anti-β3-tubulin (TUJ1) (Santa Cruz Biotechnology, Santa Cruz, CA, USA) and anti-microtubule associated protein-

2 and 5 (-Map2 and -Map5, respectively) (Abnova, Taipei, Taiwan), anti-O4, anti-chondroitin sulfate proteoglycan (-NG2), anti-gial fibrillary acidic protein (-GFAP) (Millipore, Billerica, MA, USA). Following overnight incubation at 4°C, cells were washed with PBS and stained with Alexa-Fluor-594nm conjugated secondary antibodies (Molecular Probes-Invitrogen; www.invitrogen.com) for 1h at room temperature, after which the cover slips were mounted and the nuclei counterstained with Vectashield with DAPI (Vector Laboratories Inc., Burlingame, CA, USA). Negative controls were processed under the same experimental conditions minus primary antibodies. Images were acquired by fluorescence microscopy (Eclipse-TE2000-S, Nikon, Tokyo, Japan) using the F-ViewII FireWire™ camera (Soft Imaging System, Olympus, Tokyo, Japan) and elaborated with the Adobe Photoshop CS2 program.

Cell differentiation was assessed by counting the number of cells expressing specific markers within randomly distributed groups of 80 DAPI-stained cells selected using the Cell<sup>^</sup>F software (Soft Imaging System, Olympus).

### BrdU incorporation assay

BrdU (5-Bromo-2'-deoxyuridine) incorporation was determined at specific time points in stem cells grown on glass cover slips, TCP, a-C:H and patterned substrates in the presence/absence of BDNF. The cells were pulsed with 10μM BrdU for 5h at 37°C in a humidified incubator with 5% CO<sub>2</sub>. The procedure was carried out as recommended by the manufacturer (BD Pharmingen™, Franklin Lakes, NJ, USA). Briefly, fixed cells were permeabilized and blocked with a solution composed of PBS, 0.5% Tween 20 (Sigma) and 10% FBS, then washed with PBS and exposed to 100 U/mL DNase I recombinant/ RNase-free (Roche; www.roche.com). Cultures were stained with a mouse, anti-BrdU monoclonal antibody (BD Bioscience) in PBS, 0.5% Tween 20 and FBS 1% overnight at 4°C. After washing with PBS, cells were stained with a goat anti-mouse Alexa488-conjugated secondary antibody (Molecular Probes-Invitrogen) for 1h at room temperature. The cover slips were mounted and the nuclei counterstained with Vectashield with DAPI (Vector Laboratories.). Images were acquired by fluorescence microscopy (Eclipse-TE2000-S, Nikon) using an F-ViewII FireWire™ camera (Soft Imaging System, Olympus).

### Elongation characterization

To evaluate cell elongation factors, measurements were performed on day 12 of culture for each substrate (TCP, a-C:H films, and micropatterned nanoridges). As carried out in previous studies (Martino *et al.*, 2009a), eight different areas were photographed (20-40X magnification). The images were analyzed with the Cell<sup>^</sup>F View image software (Soft Imaging System, Olympus). The elongation (*E*) factor reflects the extent of the equimomental ellipse (Yim *et al.*, 2005). The *E* factor is defined as the ratio between long and short axis minus 1. Thus, *E*=0 for a circle, and *E*=1 for an ellipse with an axis ratio of 0.5. For each condition an average of 300 cells was analyzed.

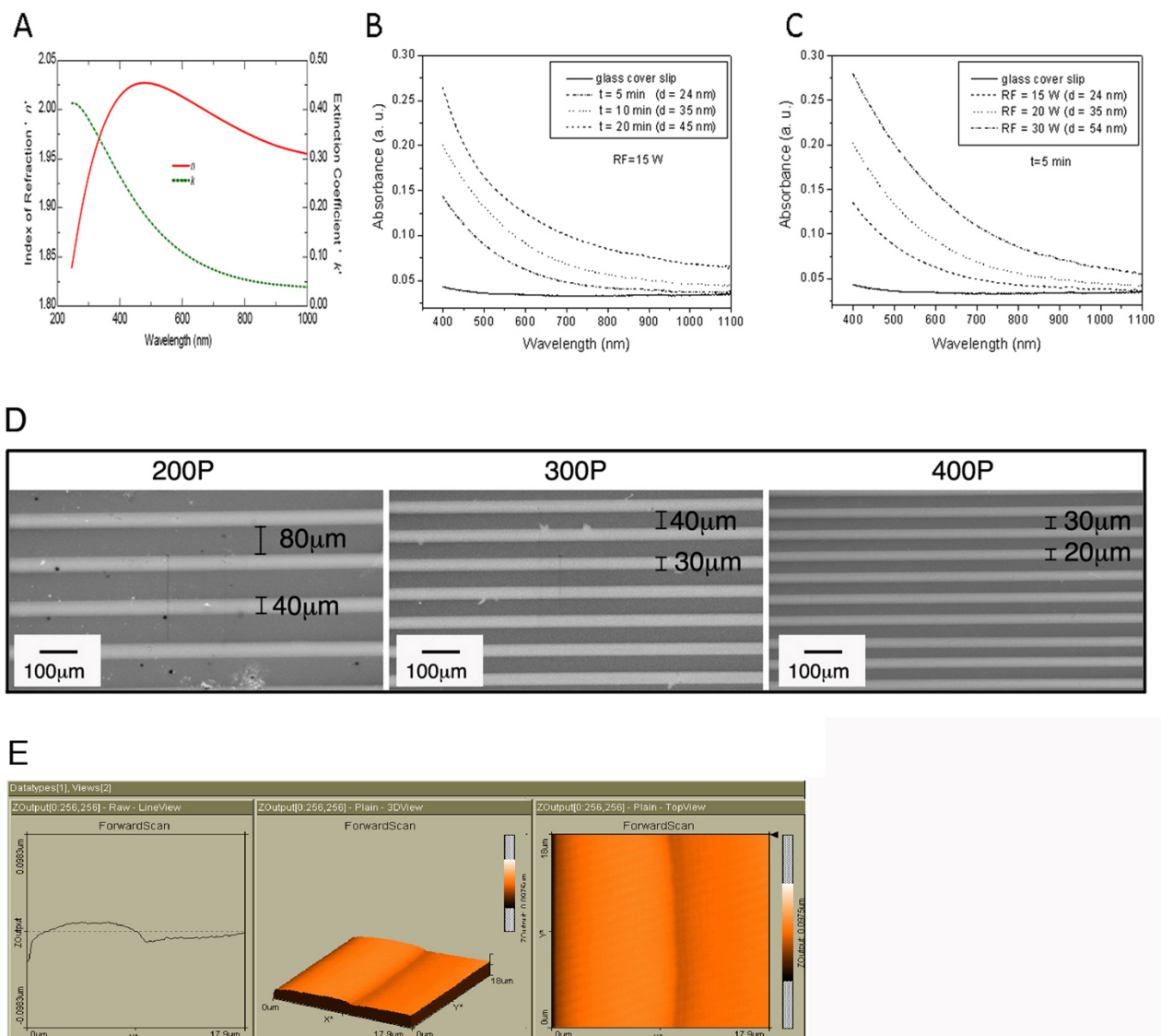


**Fig. 1.** a-C:H micropatterned nanoridges characterization. **(A)** Optical constant of a-C:H vs wavelength. **(B)** Optical absorption curves of a-C:H film obtained with variable power supply. **(C)** Optical absorption curves of a-C:H film obtained with variable deposition time. **(D)** FESEM images of a-C:H ridges obtained by using a 200P; 300P and a 400P mask. **(E)** AFM images of line view, 3D and 2D topography of 300P amorphous carbon patterned film.

### Neurite-like length measurement

Neurite-like length measurement was performed on TUJ1 immune-labeled cultures based on a protocol from Li *et al.* (2008), with a few modifications. Following 12 days of culture on different substrates (glass cover slip, TCP, uniform a-C:H, and patterned a-C:H) in serum-free medium with/without BDNF, measurements were performed using digital images taken from a Nikon TE2000S microscope in epi-fluorescence mode equipped with an Olympus camera (20x magnification). Captured images were processed and analyzed with the Cell<sup>F</sup> View image software (Soft Imaging System, Olympus).

Protrusions of TUJ1-positive cells with bipolar asymmetric shape were considered “neurite-like” if longer than 80  $\mu\text{m}$ . In the case of branched protrusions, measurements were performed on the longest neurite branch. Ridges and, in their absence, the horizontal axis of smooth surfaces (glass, TCP and uniform a-C:H film) were used as a reference for alignment purposes. Results

are expressed as mean neurite-like length ( $\mu\text{m}$ )  $\pm$  SEM. For each condition an average of 300 cells was analyzed.

### Protein adsorption

Protein adsorption assessments were performed by transferring 300 $\mu\text{g}$  of bovine serum albumin (BSA) (Sigma-Aldrich), human plasma from healthy donors (obtained with informed consent) or 10% FBS culture medium onto uniform a-C:H, 200P, 300P, 400P pattern films, glass cover slips and TCP. Proteins were incubated for either 30 min (according to Yang *et al.*, 2003; Popov *et al.*, 2009; Valsichina *et al.*, 2009) or 24 hr at 37°C. After three washing steps in H<sub>2</sub>O total protein content was measured by the Bradford method (Bradford, 1976) using bovine serum albumin as the standard. Absorbance (595nm) was measured using a microtiter plate reader (ELISA reader, GDV-DV990BV6, Italy). Every sample was analyzed in five independent experiments, each of which run in triplicate.

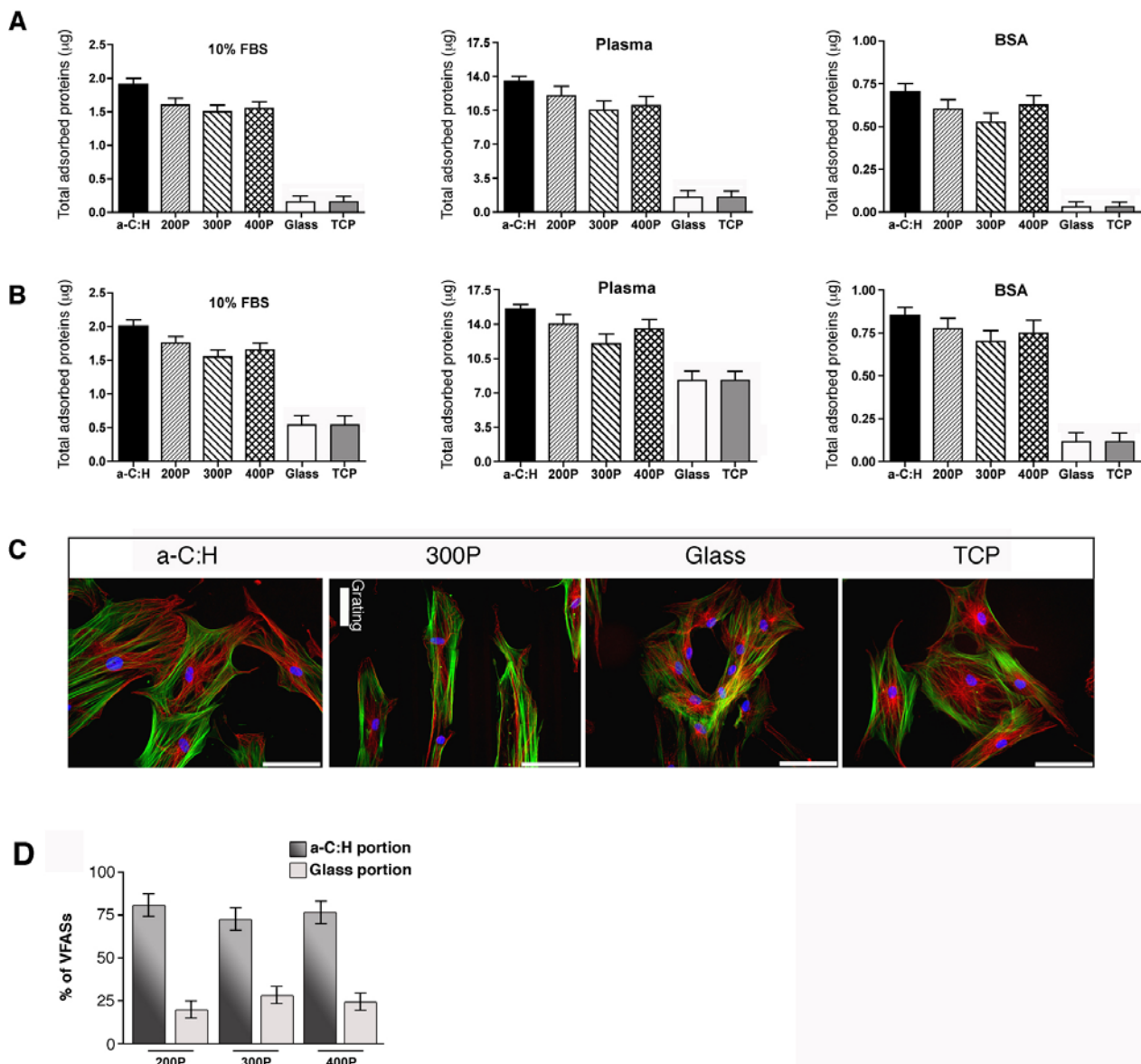


**Fig. 2.** hBM-MSCs and a-C:H micropatterned nanoridges surfaces interaction. **(A, B)** Total adsorbed proteins ( $\mu$ g) from 10%FBS, human plasma and BSA on uniform a-C:H, a-C:H patterned substrates (200P, 300P and 400P), glass and TCP after 15 min at 37°C **(A)**, and 24hr at 37°C **(B)**. Data are from a representative experiment chosen out of five which yielded similar results. Results are expressed as mean  $\pm$ SEM. **(C)** Representative images of hBM-MSCs seeded on a-C:H thin film, 300P a-C:H patterned glass cover slips, glass cover slips and tissue culture polystyrene (TCP). Microtubule organization is shown by  $\alpha$ -tubulin (TRIC)/F-actin (fluorescein isothiocyanate (FITC))/4',6-diamidino-2-phenylindole (DAPI) staining. Images were captured with 20X objectives; scale bar: 100  $\mu$ m. **(D)** Percentage of VFASs per cell seeded on a-C:H or glass portion. Cell adhesion was quantified by counting the number of vinculin focal adhesion spots (VFASs) per cell in cells grown on a-C:H portion and glass portion of micropatterned films. Data are from a representative experiment chosen out of five which yielded similar results. Results are expressed as mean  $\pm$ SEM.

### Cell adhesion quantification

Cell adhesion was quantified by evaluating the number of vinculin focal adhesion spots (VFASs) per cell 24hr and 72hr after seeding (Martino *et al.*, 2009a). To this end, 80 cells were analyzed in each test with the CellF software (Soft Imaging System, Olympus).

### Field emission scanning electron microscopy (FESEM)

Cell-material interactions were evaluated using field emission scanning electron microscopy (FESEM) (Supra

25, Zeiss) after 12 days of culture. Cells were washed twice with PBS and fixed in 2.5% glutaraldehyde for 30 min at room temperature. Samples were dehydrated with increasingly concentrated ethanol solutions (5-100%, v/v) dispensed every 5 min, followed by a critical point drying process (Emitech K850, Quorum Technologies, East Grinstead, UK). Once dried, samples were sputter coated with 15nm gold and then subjected to FESEM at an accelerating voltage of 5kV.

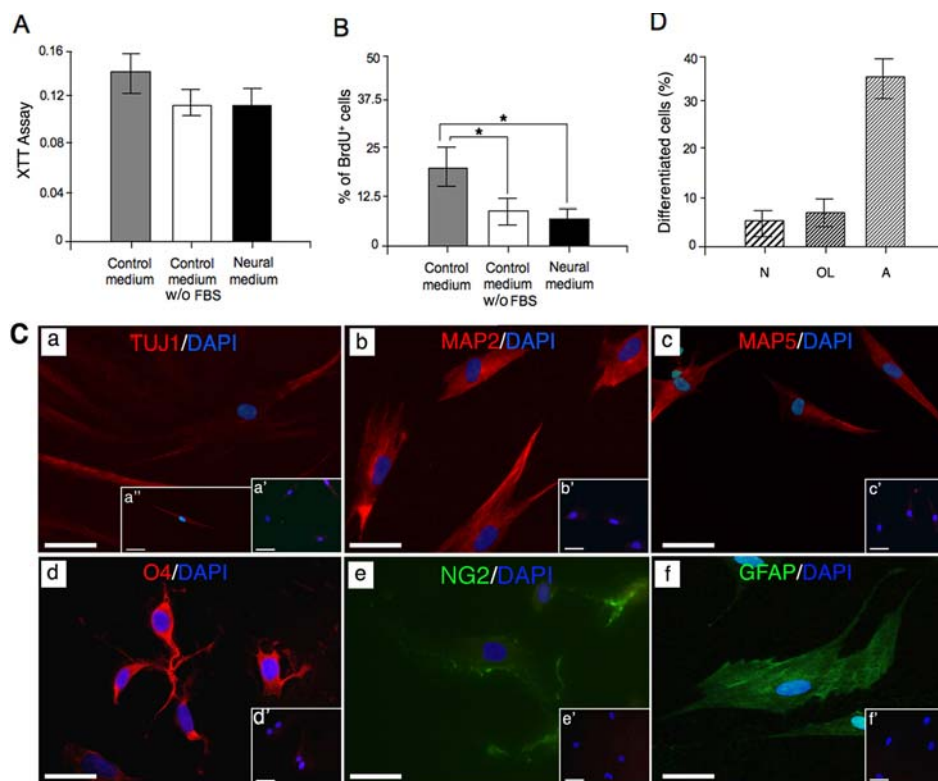


**Fig. 3.** Differentiation of hBM-MSCs toward astrocytes, oligodendrocytes and neurons. hBM-MSCs were cultured on TCP in the presence of a mixture of factors (BDNF, bFGF, PDGF-AA) for 12 days. **(A)** XTT viability assay of hBM-MSCs plated on TCP and cultured in control medium with FBS, control medium without FBS and neural medium. **(B)** BrdU incorporation assay of cells seeded on TCP and cultured as described above. \*Denotes significant difference ( $p < 0.05$ ). **(C)** Immunofluorescence analysis. Cells were stained for TUJ1, MAP2, MAP5, O4, NG2 and GFAP (a-f, a'' neural medium treated and a'-f' control medium treated, respectively). Cell nuclei (blue) were stained with DAPI. **(D)** Percentage of differentiated cells, N=neuronal, OL=Oligodendrocytes, A=Astrocytes. Data are expressed as percentages of cells immunoreactive for each marker in relation to the total number of cells and represent the mean $\pm$ SEM from five independent experiments performed in triplicate. Scale bar: 50 $\mu$ m.

### Statistical analysis

Data are presented as the mean value  $\pm$  standard error of the mean (SEM). One-Way ANOVA test (Prism version 4, 2004 edition; GraphPad, La Jolla, CA, USA) was used for statistical analyses, with  $p < 0.05$  considered significant.

## Results

### a-C:H micropatterned nanoridge characterization

The a-C:H films obtained with a 15 W power supply and 5 min treatment time showed a thickness of 24 nm and a refractive index typical of amorphous carbon (Fig. 1A). This outcome was chosen as a reference value to evaluate film thickness under any deposition conditions.

The optical density of glass cover slips and a-C:H films is shown in Fig. 1B and Fig. 1C, respectively. In this regard, curves consistently displayed markedly high absorbance values across a broad spectral region (400-1000 nm) in relation to both deposition time under constant RF (Fig. 1B) and power supply under constant treatment time (Fig. 1C). Based on the thickness value obtained after 5 min deposition, we calculated the film thickness, as obtained with different deposition parameters, at a fixed wavelength of 550 nm. The a-C:H thickness ranged from 24 to 54 nm

when RF increased from 15 to 30 W, while a-C:H thickness ranged from 24 to 45 when the treatment time increased from 5 to 20 min (Fig. 1).

For the development of micropatterned nanoridges, we chose an a-C:H film with a thickness of 24 nm to ensure higher stability. Wettability analysis revealed that deposited a-C:H coating had a contact angle of  $77 \pm 1^\circ$  compared to distilled water. Further, we estimated the surface free energy of the film to be 51.15 mN/m, in agreement with previous studies (Martino *et al.*, 2009a; Popov *et al.*, 2009; Vasilchina *et al.*, 2009).

The ridge dimensions for the three different masks were measured by FESEM (Fig. 1D). The darker, parallel areas revealed a-C:H micropatterned nanoridges deposited on glass substrate. The a-C:H ridge average dimensions (width/spacing) were 80/40  $\mu$ m (200P), 40/30  $\mu$ m (300P) and 30/20  $\mu$ m (400P), respectively (Fig. 1D), as determined by analyzing micrographs. The percentage of area covered by amorphous carbon film changed in relation to ridge geometry and was found to decrease from 200P>400P>300P (67%, 60%, 57%).

The morphology appeared to be regular and reproducible for each mask configuration. AFM images show the line view and the topography in 3D and 2D of the transition between amorphous carbon and the glass

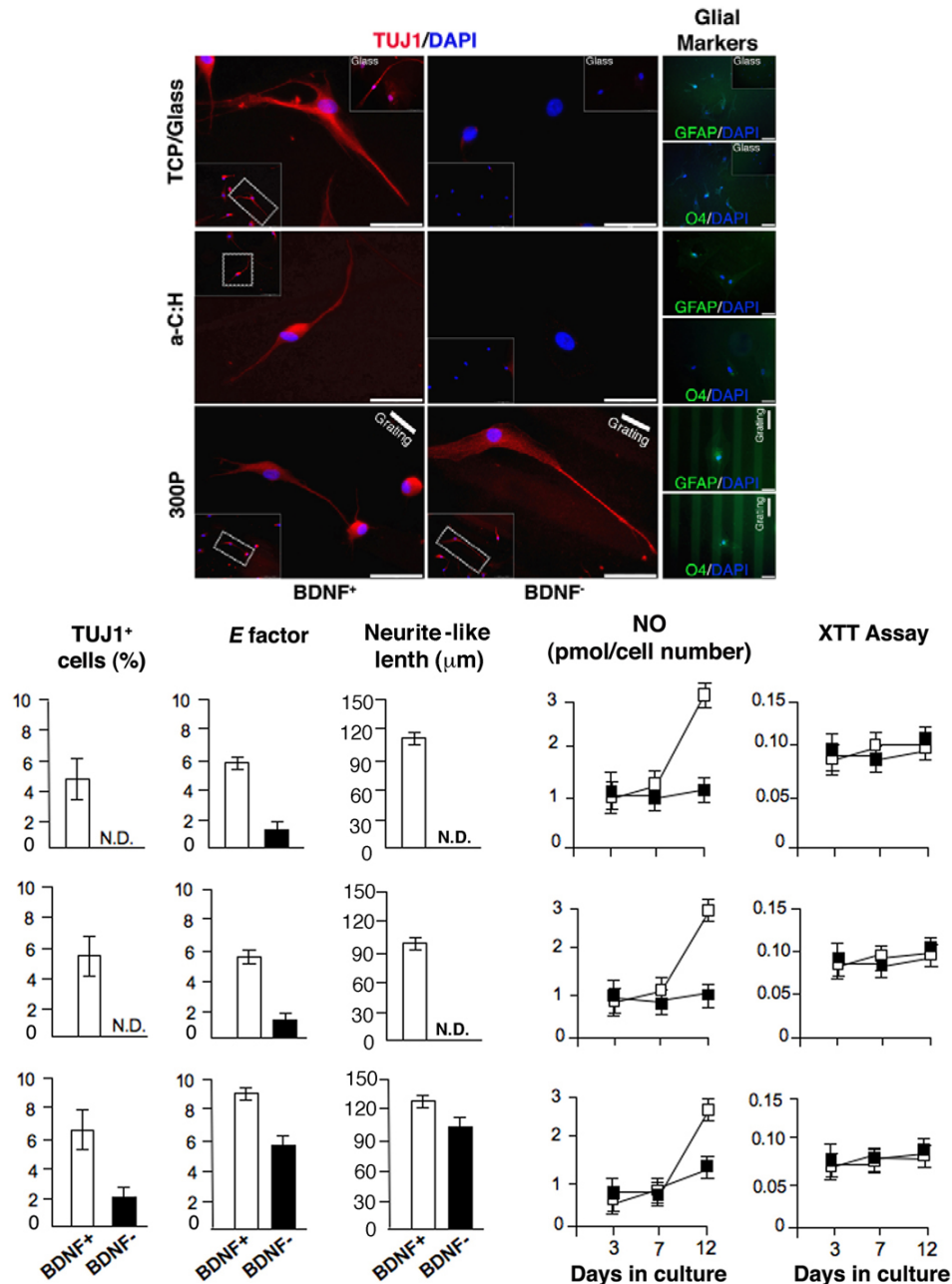


**Fig. 4.** Neuronal induction of hBM-MSCs on a-C:H micropatterned nanoridges. hBM-MSCs were cultured on different substrates: TCP/Glass, a-C:H (uniform a-C:H coating), 300P (300P micropatterned nanoridge substrates) in the presence  $\square$  /absence  $\blacksquare$  of BDNF for 12 days.

**TUJ1/DAPI:** Immunofluorescence showed cells stained for TUJ1 (TRIC). Cell nuclei (blue) were stained with DAPI.

**Glial markers:** Immunofluorescence showed cells stained for GFAP and O4. Nuclei (blue) were stained with DAPI.

**TUJ1<sup>+</sup> cells:** Percentage of differentiated cells expressing the TUJ1 marker. Data are expressed as percentages of cells immunoreactive for the marker in relation to the total number of cells and represent the mean  $\pm$  SEM from five independent experiments performed in triplicate.

**E factor:** Elongation factor (Yim *et al.*, 2005) was measured for cells cultured on each substrate for 12 days in the presence  $\square$  /absence  $\blacksquare$  of BDNF.

**Neurite-like length:** The longest protrusion of bipolar cells (neurite-like) was measured in TUJ1-positive cells grown on each substrate in the presence  $\square$  /absence  $\blacksquare$  of BDNF (See Materials and Methods section for measurement details).

**NO:** Nitric oxide released by hBM-MSCs grown on TCP, uniform a-C:H and 300P a-C:H ridges for 3, 7 and 12 days in the presence  $\square$  /absence  $\blacksquare$  of BDNF. Data are expressed as ratios between pmol NO (released) and cell number.

**XTT:** XTT viability test for hBM-MSCs seeded on TCP, uniform a-C:H and 300P a-C:H ridges and grown in the presence  $\square$  /absence  $\blacksquare$  of BDNF). Scale bar: 50  $\mu$ m.

Results are expressed as mean  $\pm$  SEM. Data shown are representative for five independent experiments.

**Table 1.** Cell adhesion on a-C:H micropatterned nanoridges surfaces.

Substrates	VFASs per cell at 24hr	VFASs per cell at 72hr
a-C:H	104±6	138±11
200P	66±2 <sup>a</sup>	86±2 <sup>a</sup>
300P	68±4 <sup>a</sup>	78±8 <sup>a</sup>
400P	74±4 <sup>a</sup>	84±4 <sup>a</sup>
Glass	106±8	130±9
TCP	95±8	137±12

Cell adhesion was assessed by counting the number of vinculin focal adhesion spots (VFASs) per cell. Data are representative of five independent experiments; results are expressed as mean ± SEM. Statistical significance was determined through one-way ANOVA test with Bonferroni's multiple comparison test (Prism version 4, 2004 edition; GraphPad). \* $p < 0.05$  vs uniform a-C:H

portion in 300P nanopatterned films assembled on glass cover slips (Fig. 1E). Surface properties underlined a uniform roughness of the films and a steep transition that is representative of all of the mask configurations. Wettability analysis revealed a water contact angle on 200P, 300P and 400P patterned surfaces of  $69 \pm 1^\circ$  and the surface free energy of 53.8 mN/m in all configurations.

#### a-C:H micropatterned nanoridges, protein adsorption and cell adhesion

First we evaluated the effect of the patterned a-C:H (200P, 300P and 400P) surface chemistry and topography on protein adsorption (Fig. 2A, 2B). As a control, we measured protein adsorption on uniform a-C:H, glass cover slips and TCP. We employed as protein sources human plasma from healthy donors (according to Popov *et al.*, 2009; Vasilchina *et al.*, 2009), 10% FBS and purified BSA (Fig. 2A, 2B).

The results show that protein adsorption was higher for plasma as compared to 10% FBS and much higher as compared to BSA. The quantity of protein adsorption was in the order: uniform a-C:H > nanopattern a-C:H (200P  $\cong$  400P  $\cong$  300P) > glass cover slip and TCP (Fig. 2A). This trend was maintained after 24 hr of incubation, although we measured minor increases of protein adsorption with 10% FBS, plasma and BSA on uniform a-C:H and micropatterned a-C:H (200P, 300P, 400P), and more significant increases on glass cover slips and TCP (Fig. 2B).

We compared these results with those obtained by measuring cell adhesion after 10% FBS protein adsorption on each surface. As already reported (Martino *et al.*, 2009a), hBM-MSCs cultured on RPMI containing 10% FBS showed comparable cell growth rates and cell viability and an absence of cytotoxicity on both uniform and patterned a-C:H coatings as well as on glass and TCP (data not shown; Martino *et al.*, 2009a). Notably, we confirmed that stem cells assumed an elongated morphology only on the ridge patterned films, whereas cells maintained a fibroblast-like morphology on smooth surfaces (uniform a-C:H, TCP and glass) (Fig. 2C). Representative images showed cells elongated in the direction of ridge topography, although the elongation was highest on ridge 300P (Fig. 2C; Martino *et al.*, 2009a).

It is well known that the number of VFASs reflects the number of contacts between cellular membrane and

substrate and, consequently, molecular interactions with the different surfaces (Curtis, 2004; Diener *et al.*, 2005; Keselowsky and Garcia 2005). We did not observe the formation of VFASs in cells seeded on any substrate after 30 min (data not shown). After 24hr, we found well organized VFASs. Notably, the number of VFASs decreased in the order: uniform a-C:H > glass cover slip and TCP > micropatterned a-C:H, indicating that even the lowest level of FBS protein adsorption on glass and TCP was sufficient to induce cell adhesion mechanisms in a comparable manner regardless of the surface type (Table 1). After 72hr, although the trend was maintained, we observed an increase of VFAS per cell on all surfaces (Table 1). Remarkably, we confirmed our previous observation that the VFASs on the ridge topography were significant higher on the lines of a-C:H as compared to the interspersed stripes of glass (Fig. 2D, Martino *et al.*, 2009a).

#### Differentiation of hBM-MSCs toward astrocytes, oligodendrocytes and neurons

We first evaluated the multipotentiality of hBM-MSCs toward neural lineages, by inducing hBM-MSCs to differentiate toward astrocytes, oligodendrocytes and neurons according to established protocols (Prockop, 1997; Sanchez-Ramos, 2002; Stewart and Przyborski, 2002; Grove *et al.*, 2004; Dezawa *et al.*, 2004; Magaki *et al.*, 2005; Bonilla *et al.*, 2005; Engler *et al.*, 2006).

hBM-MSC cultured on TCP for twelve days in the presence of a mixture of trophic factors (135ng  $\beta$ -FGF, 50ng BDNF, 10ng PDGF-AA) and in the absence of FBS showed no signs of toxicity or cell stress as indicated by levels of dehydrogenase activity that were comparable to cells grown under standard conditions (Fig. 3A). All differentiated cells were BrdU-negative, suggesting that the majority of induced neural cells were post-mitotic (Fig. 3B). Treatment with a mixture of trophic factors resulted in the efficient generation of a heterogeneous, differentiated cell population. These cells expressed high levels of neuronal markers, oligodendrocytes and astrocytes, (TUJ1, MAP2-ab, MAP5-ab, O4, NG2, and GFAP respectively; Fig. 3C) but did not have a conventional neural morphology (Fig. 3C). Quantification of this data indicated that approximately 6% of these cells expressed neuronal markers, namely TUJ1, MAP2-ab, MAP5-ab, while 8% of the cells expressed oligodendrocyte markers (O4 and

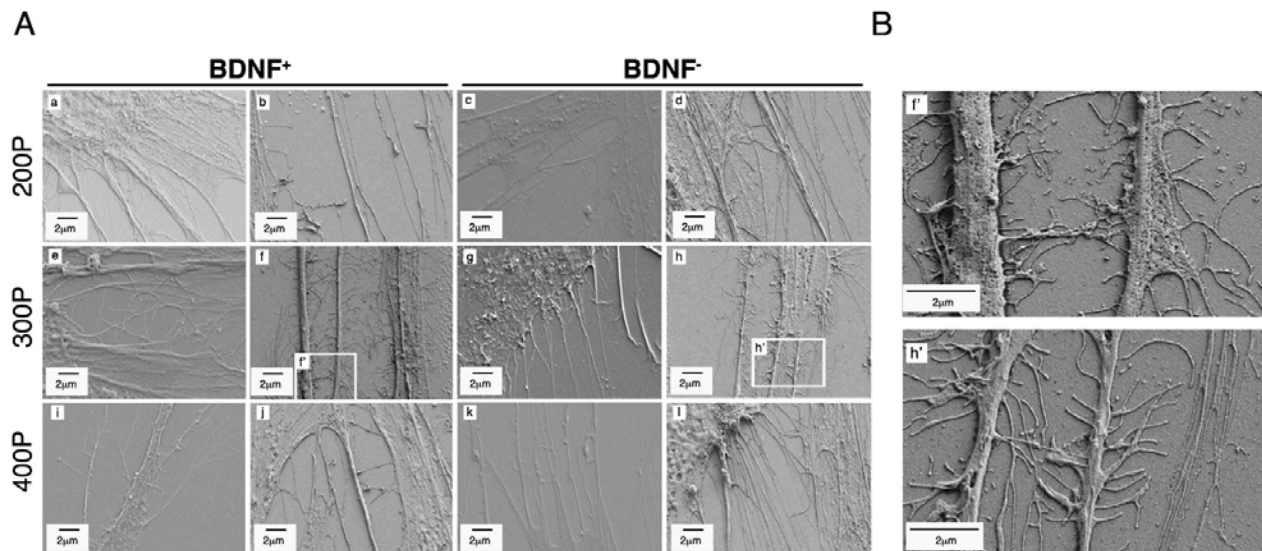


**Fig. 5.** FESEM analyses. **(A)** FESEM images showing the interaction of hBM-MSCs with 200P, 300P and 400P nanopatterned a-C:H films in the presence/absence of BDNF. **(B)** Higher magnification of images shown in two inset boxes of panel A depicting hBM-MSCs interactions with 300P micropatterned a-C:H nanoridges in the presence/absence of BDNF.

NG2) and 35% of cells were positive for the astrocyte marker GFAP (Fig. 3D). Cells cultured in control medium w/o FBS were, instead, negative for the markers investigated (Fig. 3C, a'-f').

Thus, these findings are in agreement with the rate of neural differentiation obtained from other stem cell types (embryonic stem cells, neural stem cells, induced pluripotent stem cells) (Engler *et al.*, 2006; Hu *et al.*, 2009; Kim *et al.*, 2009; Martino *et al.*, 2009b).

#### Neuronal induction of hBM-MSCs on a-C:H nanotopographies

To investigate whether the patterned a-C:H films induce neuronal differentiation of stem cells as a single stimulus, we cultured hBM-MSCs on a-C:H micropatterned nanoridges with different dimensions (200P, 300P, 400P) in serum free-conditions (BDNF<sup>-</sup> culture). As a control, we replicated these experiments in the presence of soluble BDNF employed as a biochemical stimulus (BDNF<sup>+</sup> culture). Comparative experiments were conducted on uniform a-C:H, TCP and glass cover slips.

We monitored the neuronal differentiation process by counting the number of cells positive for the neuronal marker TUJ1<sup>+</sup> that is expressed as terminal differentiated neural cells (Horne *et al.*, 2009; Prabhakaran *et al.*, 2009). We also measured the levels of released nitric oxide as a parameter of neuronal differentiation (Cappelletti *et al.*, 2003; Cheng *et al.*, 2003). Furthermore, we measured the elongation factor (*E*) and the length of the longest cellular protrusion (neurite-like) to evaluate the differences in morphology that occur in cell cytoskeleton architecture (Li *et al.*, 2008; Jin *et al.*, 2008; Yim *et al.*, 2005; Zhu *et al.*, 2004). Finally we measured dehydrogenase activity to assess cell viability.

#### hBM-MSCs, BDNF and TCP/Glass cover slips

First, we explored whether the single administration of BDNF for 12 days was sufficient to induce neuronal differentiation of hBM-MSCs (Fig. 4, lines TCP/Glass).

On both substrates, we found that administration of soluble BDNF induced hBM-MSCs to acquire a predominantly neuronal morphology, featuring a small cell body and extended bipolar neurite-like processes with abundant varicosities (Fig. 4, line TCP/Glass). Treated cells that expressed the marker TUJ1 ( $4.9 \pm 1.2\%$  with respect to total cells), displayed an elongation factor (*E*) of  $6.0 \pm 0.3$ , a major neurite-like process length of  $109 \pm 15 \mu\text{m}$ , and, as expected, a significant enhancement of NO levels compared to untreated cells (Fig. 4, line TCP/Glass; TUJ1; *E* factor; neurite-like length; NO).

No TUJ1<sup>+</sup> cells were detected on BDNF<sup>-</sup> cultures (Fig. 4, line TCP/Glass, TUJ1). Moreover, under these culture conditions, cells showed a lower *E* factor ( $E = 1.2 \pm 0.2$ ), had short cellular protrusions and low NO levels compared to the BDNF-treated cells (Fig. 4, line TCP/Glass; *E* factor; neurite-like length; NO). No expression of the glial markers O4 and GFAP was detected in BDNF<sup>+</sup> and control cultures (Fig. 4, line TCP/Glass, Glial markers). Finally, no signs of cytotoxicity were observed in either treated or control cultures (Fig. 4, line TCP/Glass, XTT).

#### hBM-MSCs, BDNF and uniform a-C:H film.

Administration of BDNF to uniform a-C:H cultures induced morphological changes in hBM-MSCs and expression of the TUJ1 marker (Fig. 4, line a-C:H, TUJ1). TUJ1-positive cells were  $5.8 \pm 1.2\%$  with respect to total cell population. No TUJ1<sup>+</sup> cells were detected in BDNF<sup>-</sup> cultures (Fig. 4, line a-C:H, TUJ1) and no O4 and GFAP expression was detected in either BDNF-treated or untreated cell cultures (Fig. 4, line a-C:H, Glial markers).

BDNF-treated cells had a small cell body and bipolar neurite-like processes (the longest was  $110 \pm 13 \mu\text{m}$  length) with an *E* factor of  $5.5 \pm 0.3$ . Conversely, in the absence of BDNF, cellular protrusions were undetectable and the *E* factor was  $1.1 \pm 0.2$  (Fig. 4, line a-C:H: neurite-like length; *E* factor). Furthermore, levels of NO released in BDNF<sup>+</sup> cells were comparable to TCP differentiated cells, yet they were undetectable in untreated cultures (Fig. 4, line a-C:H,

NO), while cell viability was comparable to that of control cells (Fig. 4, line a-C:H, XTT).

### hBM-MSCs, BDNF and a-C:H micropatterned nanoridges

To examine whether the a-C:H micropatterned nanoridges induced hBM-MSCs to acquire neuronal phenotype as a single stimulus, we cultured hBM-MSCs on 200P, 300P and 400P ridges substrates in serum-free medium (BDNF<sup>-</sup> culture). As a control, experiments were performed in the presence of soluble BDNF (BDNF<sup>+</sup> culture).

hBM-MSC treated with/without BDNF for 12 days interacted with 200P, 300P and 400P micropatterned nanoridges, showing an elongated shape with tiny interconnecting protrusions as shown by FESEM images (Fig. 5A). Notably, in both BDNF<sup>+</sup> and BDNF<sup>-</sup> 300P cultures, we detected a more organized structure longitudinal to the ridge direction, which was absent in 200P and 400P cultures (Fig. 5B). These differences were confirmed by the different response of the stem cells to the differentiation process. While BDNF<sup>+</sup> 200P and 400P cultures resulted in 4.5±0.9% and 4.7±0.7% TUJ1<sup>+</sup> expression respectively, cells seeded on BDNF<sup>+</sup> 300P showed a significant increase in differentiated cells (6.2±0.8%; Fig. 4, line 300P, TUJ1). Remarkably, we detected 2.0±0.5% of TUJ1<sup>+</sup> cells on 300P coated substrates (as a single stimulus) without BDNF administration (Fig. 4, line 300P) whereas TUJ1<sup>+</sup> cells were only slightly detectable on 200P and 400P patterns (0.2±0.1% and 0.3±0.2%, respectively). O4 and GFAP markers were undetectable in all culture conditions (Fig. 4, line 300P, Glial markers).

After BDNF treatment, cells on 300P a-C:H ridges presented a higher *E* factor compared to the untreated 300P cultures ( $E = 8.8 \pm 0.4$  vs  $E = 6.0 \pm 0.4$ ). Both *E* values, however, were higher compared to BDNF<sup>+</sup> cells on 200P and 400P ( $E = 5.7 \pm 0.4$  and  $E = 5.5 \pm 0.3$  respectively), on smooth surfaces (Fig. 4, lines: TCP/Glass, a-C:H), and were much higher compared to the BDNF<sup>-</sup> cultures (200P:  $E = 3.4 \pm 0.4$  and 400P:  $E = 3.6 \pm 0.4$ ; TCP/Glass:  $E = 1.2 \pm 0.2$ ; a-C:H:  $E = 1.1 \pm 0.2$ ).

We observed cells with bipolar shape on 300P as well as on 200P and 400P ridge topographies following soluble BDNF treatment. Here, the neurite-like lengths were 130±15 μm, 95±9 μm and 93±8 μm, respectively. Remarkably, we observed bipolar cells and measured a neurite-like length of 95±10 μm in a-C:H 300P cultures in the absence of BDNF (Fig. 4, line 300P, neurite-like length). Conversely, bipolar cells were absent in 200P and 400P cultures without BDNF administration.

Levels of NO released by 300P, as well as by 200P and 400P BDNF-treated cells were comparable to the levels secreted by differentiated cells on TCP and a-C:H cultures (Fig. 4, line 300P, NO). Notably, increases of NO were observed on 300P BDNF<sup>-</sup> cells (Fig. 4, line 300P, NO), whereas NO measurement was undetectable on 200P and 400P ridge untreated cultures (data not shown), thus confirming the effect of the 300P topography on the neuronal induction of hBM-MSCs. Finally, levels of dehydrogenase activity were similar to those of cells grown on TCP and uniform a-C:H (Fig. 4, line 300P, XTT).

## Discussion

Here, we show that a-C:H micropatterned nanoridges and soluble BDNF orchestrate hBM-MSCs differentiation towards neuronal lineages. Further, our findings reveal that surface topography designs may induce a stem cell response by acting as a single stimulus.

Based on the highest number of TUJ1-positive cells (6.2±0.8), the highest *E* value (8.8±0.4), the longest neurite-like process and the largest increase of NO levels in the culture medium, we observed that optimal differentiation outcomes were achieved by employing 300P, (40/30 μm) a-C:H ridges in combination with a biochemical stimulus exerted by soluble BDNF (in absence of FBS in the culture medium).

Nitric oxide plays a role as a modulator of neuronal function in neurotransmitter release, synaptic plasticity, excitability, and learning (Cappelletti *et al.*, 2003); in addition, nitric oxide was shown to mediate the transition of neural precursor cells from proliferation to differentiation, likely by acting as a suppressor of DNA synthesis (Peunova *et al.*, 2001; Baskey *et al.*, 2002). Furthermore, other authors have demonstrated that NO, evoked by BDNF signaling in newly generated neurons, acts as a paracrine messenger that controls the proliferation and differentiation of neural precursor cells (NPCs) (Cheng *et al.*, 2003), suggesting that NO mediates the neurogenic effect of BDNF and, in turn, that increased levels of NO are indicative of neuronal differentiation (Cheng *et al.*, 2003).

This was indeed recapitulated by our findings, in light of a clear correlation between high levels of NO released by TUJ1 positive cells and hBM-MSC differentiation toward neuronal lineages.

Interestingly, in 300P cultures without differentiating agent conditions (thereby the topography was the unique cue), we observed 2.0±0.5% TUJ1<sup>+</sup> cells, which accounted for approximately 40% of the neural-induced cells grown on TCP/Glass cultures in the presence of BDNF. We also noted that neural cells obtained through a single mechanical stimulus displayed long neurite-like protrusions, increased levels of NO, and *E* values comparable to those measured on smooth surfaces in the presence of BDNF.

Together, these observations confirm that the 300P topography is sufficient to appropriately induce cellular elongation (Martino *et al.*, 2009a) and, more in general, trigger cell signaling associated with the development of neuronal phenotypes.

a-C:H micropatterned nanoridges formatted as 200P, 300P and 400P substrates share steep transitions between hydrogenated amorphous carbon and the glass portion, display identical height of 24 nm and different widths, namely 80/40 μm (200P), 40/30 μm (300P) and 30/20 μm (400P). The percentage of area covered by a-C:H films decreases in the order 200P>400P>300P, corresponding to 67%, 60%, 57%, with the glass portion changing accordingly (33%, 40% and 43%, respectively). However, comparable water contact angle, surface energy values and adsorption of proteins on 200P, 300P and 400P indicated that the chemical surface characteristics of different a-C:H ridge formats were similar. Remarkable these parameters

diverge from uniform a-C:H film, suggesting that micropatterning influenced the a-C:H surface properties (Jung and Bhushan, 2006). Therefore, the active role of the 300P a-C:H coating on stem cell neural differentiation could be a consequence of the specific nano/micropattern (24 nm step, 40  $\mu\text{m}$  width/30  $\mu\text{m}$  spacing).

It is possible that 300P a-C:H micropatterned nanoridges coordinate directional cues and guide hBM-MSCs alignment and orientation, perhaps through "contact guidance", thereby influencing the process of cell differentiation. This phenomenon is highlighted in cells cultured in the absence of soluble neurotrophic factor. In fact, ridges with 200P and 400P dimensions as single stimuli were "poor-inducers", since the percentage of TUJ1<sup>+</sup> cells obtained on those substrates was lower than 0.2%. We speculate that, in these cases, 200P and 400P contact guidance was not the dominant stimulus, probably due to ridge dimensions unsuitable for these types of cells. However, BDNF administration to 200P and 400P cultures induced neuronal differentiation to a level comparable to that obtained on smooth surfaces (TCP/Glass, a-C:H).

Conversely, the pattern dimension of 300P, in the absence of BDNF, drove hBM-MSCs to express TUJ1 marker and exhibit neuronal characteristics, thereby validating the role of ridge dimensions as a physical stimulus of differentiation and suggesting that topography exerts an effect on hBM-MSCs.

We postulate that these events mimic the relatively undefined phenomenon of mechanotransduction (Curtis and Varde, 1964; Curtis, 2004; Engler *et al.*, 2006, Dalby *et al.*, 2007a; Dalby, 2009; Wang *et al.*, 2009; Biggs *et al.*, 2010) thought to be a consequence of either forces generated by cytoskeleton rearrangements alone or by cytoskeleton rearrangements that through the actin-intermediate filament could be transferred to the nucleus with attendant changes in gene expression and cell differentiation (Clark *et al.*, 1991; Ingber, 1993; Britland *et al.*, 1996; Burrige *et al.*, 1996; Rajnicek *et al.*, 1997; Eastwood *et al.*, 1998; Charras and Horton, 2002; Dalby, 2005; Yim *et al.*, 2007). More investigations are needed in order to elucidate the basic mechanisms leading to the phenomenon of neural differentiation on a-C:H patterns. These will include observation of changes in morphology, neuronal gene expression and functional activity (e.g. action potential, neurotransmitter activity). However, our evidence for a possible implication of mechanotransduction on cell differentiation, although not conclusive, should nonetheless be considered an interesting aspect related to the functional characterization of biomaterials.

### Conclusions

We demonstrate that hBM-MSCs, grown on a-C:H micropatterned nanoridges in the presence of soluble BDNF, differentiate into neuronal-like cells. This outcome was similar for ridges with width/spacing ranging between 80/40  $\mu\text{m}$  (400P), 40/30  $\mu\text{m}$  (300P) and 30/20  $\mu\text{m}$  (200P) (micrometric dimensions) and fixed height of 24nm (nanometric step).

Notably, only the surface topography with ridge width/spacing of 40/30  $\mu\text{m}$ , as single cue, was able to induce hBM-MSC differentiation in the absence of BDNF, suggesting the implication of cell signaling associated with specific mechanical features of the biomaterial.

These results are in agreement with those of other authors showing the effect of the surface properties on stem cells or other cell types (Engler *et al.*, 2006; Ruiz and Chen, 2008; Chen *et al.*, 2010). Thus, our findings may lead to the development of biomaterials suitable for neural tissue engineering through approaches based on cellular mechanotransduction processes.

### Acknowledgments

We thank Alessandro Datti, Ph.D., from the University of Perugia, for critical reading of this work. We thank Daniela De Maglie from the University of Perugia for technical support and Stefano Schutzmam, L.O.T.-Oriol Italia s.r.l. for ellipsometry measurements. We thank Hilary Giles, M.A. for language advice and proofreading.

This study was supported by the *Ministero della Salute, Italy* (grant no. RF-UMB-2006-339457 to A.O.), the *Fondazione Cassa di Risparmio di Perugia, Italy* (grant no. 2009.020.0050 to A.O. ), the *Ministero dell'Istruzione, dell'Università e della Ricerca, Italy* (grants: FIRB Idea Progettuale no. RBIP06FH7J\_002 and PRIN no. 20084XRSBS\_001 to A.O.), and the *Istituto Nazionale Biostrutture e Biosistemi*.

### References

- Baskey JC, Kalisch BE, Davis WL, Meakin SO, Rylett RJ (2002) PC12nnr5 cells expressing TrkA receptors undergo morphological but not cholinergic phenotypic differentiation in response to nerve growth factor. *J Neurochem* **80**: 501-511.
- Biggs MJ, Richards RG, Gadegaard N, Wilkinson CD, Oreffo RO, Dalby MJ (2009) The use of nanoscale topography to modulate the dynamics of adhesion formation in primary osteoblasts and ERK/MAPK signalling in STRO-1+ enriched skeletal stem cells. *Biomaterials* **30**: 5094-5103.
- Biggs MJ, Richards RG, Dalby MJ (2010) Nanotopographical modification: a regulator of cellular function through focal adhesions. *Nanomedicine* Doi:10.1016/j.nano.2010.01.009
- Bonilla S, Silva A, Valdès L, Geijo E, Garcia-Verdugo JM, Martinez S (2005) Functional neural stem cells derived from adult bone marrow. *Neuroscience* **133**: 85-95.
- Bradford MM (1976) A rapid and sensitive method for the quantitation of microgram quantities of protein utilizing the principle of protein-dye binding. *Anal Biochem* **7**: 248-254.
- Britland S, Morgan H, Wojciak-Stodart B, Riehle M, Curtis A, Wilkinson C (1996) Synergistic and hierarchical adhesive and topographic guidance of BHK cells. *Exp Cell Res.* **228**: 313-325.

- Burridge K, Chrzanowska-Wodnicka M (1996) Focal adhesions, contractility, and signalling. *Annu Rev Cell Dev Biol* **12**: 463-518.
- Cappelletti G, Maggioni MG, Tedeschi G, Macia R (2003) Protein tyrosine nitration is triggered by nerve growth factor during neuronal differentiation of PC12 cells. *Exp Cell Res* **288**: 9-20.
- Charras GT, Horton MA (2002) Single cell mechanotransduction and its modulation analyzed by atomic force microscope indentation. *Biophys J* **82**: 2970-2981.
- Chen YC, Lee DC, Tsai TY, Hsiao CY, Liu JW, Kao CY, Lin HK, Chen HC, Palathinkal TJ, Pong WF, Tai NH, Lin IN, Chiu IM (2010) Induction and regulation of differentiation in neural stem cells on ultra-nanocrystalline diamond films. *Biomaterials*. **31**: 5575-5587.
- Cheng A, Wang S, Cai J, Rao MS, Mattson MP (2003) Nitric oxide acts in a positive feedback loop with BDNF to regulate neural progenitor cell proliferation and differentiation in the mammalian brain. *Dev Biol* **258**: 319-323.
- Clark P, Connolly P, Curtis AS, Dow JA, Wilkinson CD (1991) Cell guidance by ultrafine topography *in vitro*. *J Cell Sci* **99**: 73-77.
- Curtis AS (2004) Small is beautiful but smaller is the aim: review of a life of research. *Eur Cell Mater* **8**: 27-36.
- Curtis AS, Varde M (1964) Control of cell behaviour: Topological factors. *J. Natl Cancer Res. Inst* **33**: 15-26.
- Dalby MJ (2005) Topographically induced direct cell mechanotransduction. *Med Eng Phys* **27**: 730-742.
- Dalby MJ (2009) Nanostructured surfaces: cell engineering and cell biology. *Nanomed* **4**: 247-258.
- Dalby MJ, Gadegaard N, Herzyk P, Sutherland D, Agheli H, Wilkinson C D, Curtis A S (2007a) Nanomechanotransduction and interphase nuclear organization influence on genomic control. *J Cell Biochem* **102**: 1234-1244.
- Dalby MJ, Gadegaard N, Tare R, Andar A, Riehle MO, Herzyk P, Wilkinson CD, Oreffo RO (2007b) The control of human mesenchymal cell differentiation using nanoscale symmetry and disorder. *Nat Mater* **6**: 997-1003.
- Dezawa M, Kanno H, Hoshino M, Cho H, Matsumoto N, Itokazu Y, Tajima N, Yamada H, Sawada H, Ishikawa H, Mimura T, Kitada M, Suzuki Y, Ide C (2004) Specific induction of neuronal cells from bone marrow stromal cells and application for autologous transplantation. *J. Clin. Invest* **113**: 1701-1710.
- Diener A, Nebe B, Luthen F, Becker P, Beck U, Neumann HG, Rychly J (2005) Control of focal adhesion dynamics by material surface characteristics. *Biomaterials* **26**: 383-392.
- Eastwood M, McGrouther DA, Brown RA (1998) Fibroblast responses to mechanical forces. *Proc Inst Mech Eng* **212**: 85-92.
- Engler AJ, Sen S, Sweeney HL, Discher DE (2006) Matrix elasticity directs stem cell lineage specification. *Cell* **126**: 677-689.
- Grove JE, Bruscia E, Krause DS (2004) Plasticity of bone marrow-derived stem cells. *Stem Cells* **22**: 487-500.
- Horne MK, Nisbet DR, Forsythe JS, Parish C (2009) Three dimensional nanofibrous scaffolds incorporating immobilized BDNF promote proliferation and differentiation of cortical neural stem cells. *Stem Cells Dev* doi:10.1089/scd.2009.0158
- Hu BY, Du ZW, Zhang SC (2009) Differentiation of human oligodendrocytes from pluripotent stem cells. *Nat Protoc* **4**: 1614-1622.
- Ingber DE (1993) Cellular tensegrity: Defining new rules of biological design that govern the cytoskeleton. *J Cell Sci* **104**: 613-627.
- Keselowsky B, Garcia A (2005) Quantitative methods for analysis of integrin binding and focal adhesion formation on biomaterial surfaces. *Biomaterials* **26**: 413-418.
- Jin CY, Zhu BS, Wang XF, Lu QH, Chen WT, Zhou XJ (2008) Nanoscale surface topography enhances cell adhesion and gene expression of Madine Darby canine kidney cells. *J Mater Sci Mater Med*. **19**: 2215-2222.
- Jung YC, Bhushan B (2006) Contact angle, adhesion and friction properties of micro- and nanopatterned polymers for superhydrophobicity. *Nanotechnology* **17**: 4970-4980.
- Kim JB, Greber B, Araúzo-Bravo MJ, Meyer J, Park KI, Zaehres H, Schöler HR (2009) Direct reprogramming of human neural stem cells by OCT4. *Nature* **461**: 649-653.
- Li J, McNally H, Shi R (2008) Enhanced neurite alignment on micro-patterned poly-L-lactic acid films. *J Biomed Mater Res A*. **87**: 392-404.
- Magaki T, Kurisu K, Okazaki T (2005) Generation of bone marrow-derived neural cells in serum-free monolayer culture. *Neuroscience Letters* **384**: 282-287.
- Martino S, D'Angelo F, Armentano I, Tiribuzi R, Pennacchi M, Dottori M, Mattioli S, Caraffa A, Cerulli G G, Kenny J M, Orlacchio A (2009a) Hydrogenated amorphous carbon nanopatterned film designs drive human bone marrow mesenchymal stem cell cytoskeleton architecture. *Tissue Eng Part A* **15**: 3139-3149.
- Martino S, di Girolamo I, Cavazzin C, Tiribuzi R, Galli R, Rivaroli A, Valsecchi M, Sandhoff K, Sonnino S, Vescovi A, Gritti A, Orlacchio A (2009b) Neural precursor cells cultures from GM2 gangliosidosis animal models recapitulate the biochemical and molecular hallmarks of the brain pathology. *J Neurochem* **109**: 135-147.
- Orlacchio A, Bernardi G, Orlacchio A, Martino S (2010a) Stem cells and neurological diseases. *Discov Med*. **9**: 546-553.
- Orlacchio A, Bernardi G, Orlacchio A, Martino S (2010b) Stem cells: an overview of the current status of therapies for central and peripheral nervous system diseases. *Curr Med Chem*. **17**: 595-608.
- Owens DK, Wendt RC (1969) Estimation of the surface free energy of polymers. *J Appl Polym Sci* **13**, 1741-1746.
- Palmerini CA, Arienti G, Mazzolla R, Palombari R (1998) A new assay for the determination of low-molecular-weight nitrosothiols (nitrosoglutathione), NO, and nitrites by using a specific and sensitive solid-state amperometric gas sensor. *Nitric Oxide* **2**: 375-380.
- Palmerini CA, Arienti G, Palombari R (2000) Determination of S-nitrosohemoglobin using a solid-state amperometric sensor. *Nitric Oxide* **4**: 546-549.

Palmerini CA, Arienti G, Palombari R (2003) Electrochemical determination of nitric oxide and of its derivatives. *Talanta* **61**: 37-41.

Peunova N, Scheinker V, Cline H, Enikolopov G (2001) Nitric Oxide Is an Essential Negative Regulator of Cell Proliferation in *Xenopus* Brain. *J Neuroscience* **21**: 8809-8818.

Popov C, Vasilchina H, Kulisch W, Danneil F, Stuber M, Ulrich S, Welle A, Reithmaier J.P (2009) Wettability and protein adsorption on ultrananocrystalline diamond/amorphous carbon composite films. *Diamond & Related Materials* **18**: 895-898.

Prabhakaran MP, Venugopal JR, Ramakrishna S (2009) Mesenchymal stem cell differentiation to neuronal cells on electrospun nanofibrous substrates for nerve tissue engineering. *Biomaterials* **30**: 4996-5003.

Prockop DJ (1997) Marrow stromal cells as stem cells for nonhematopoietic tissues. *Science* **276**: 71-74.

Rajnicek A, Britland S, McCaig C (1997) Contact guidance of CNS neurites on grooved quartz: influence of groove dimensions, neuronal age and cell type. *J Cell Sci.* **110**: 2905-2913.

Ruiz SA, Chen CR (2008) Emergence of Patterned Stem Cell Differentiation Within Multicellular Structures. *Stem Cells* **26**: 2921-2927.

Sanchez-Ramos RJ (2002) Neural cells derived from adult bone marrow and umbilical cord blood. *J Neurosci Res* **69**: 880-893.

Stewart R, Przyborski S (2002) Non-neural adult stem cells: tools for brain repair? *Bioessays* **24**: 708-713.

Yang P, Huang N, Leng YX, Chen JY, Fu RK, Kwok SC, Leng Y, Chu PK (2003) Activation of platelets adhered on amorphous hydrogenated carbon (a-C:H) films synthesized by plasma immersion ion implantation-deposition (PIII-D). *Biomaterials* **24**: 2821-2829.

Yim EK, Pang SW, Leong KW (2007) Synthetic nanostructures inducing differentiation of human mesenchymal stem cells into neuronal lineage. *Exp Cell Res* **313**: 1820-1829.

Yim EKF, Reano RM, Pang SW, Yee AF, Chen CS, Leong KW (2005) Nanopattern-induced changes in morphology and motility of smooth muscle cells. *Biomaterials* **26**: 5405-5413.

Vasilchina H, Popov C, Ulrich S, Ye J, Danneil F, Stüber M, Welle A (2009) Wetting behaviour and protein adsorption tests on ultrananocrystalline diamond and amorphous hydrogenated carbon thin films. *Nanostructured Materials for Advanced Technological Applications Part 4*, pp 501-508

Wang N, Tytell JD, Ingber DE (2009) Mechanotransduction at a distance: mechanically coupling the extracellular matrix with the nucleus. *Nat Rev Mol Cell Biol.* **10**: 75-82.

Zhu B, Zhang Q, Lu Q, Xu Y, Yin J, Hu J, Wang Z (2004) Nanotopographical guidance of C6 glioma cell alignment and oriented growth. *Biomaterials* **25**: 4215-4223

## Discussion with Reviewers

**Reviewer I:** These are not normal neuronal morphologies and there has been no observation of action potential. The results fit well with prior observations and MSC – neuron morphologies. However, I am not sure TUJ is a good enough marker and I think stressed MSCs taking on this odd elongate morphology may express it. Perhaps these MSCs are trying to become neurons, however, only recording of action potential can show this. Whilst still transdifferentiation, formation of glia cells is probably more likely and still interesting. Please comment.

**Authors:** We agree that the detection of stem cell differentiation in *in vitro* culture is difficult. However, many parameters could be checked. Therefore, we decided to monitor the neuronal differentiation process by counting the number of TUJ1+ cells, because this marker is expressed by terminal differentiated neuronal cells (Horne *et al.*, 2009; Prabhakaran *et al.*, 2009, text references). We also measured the level of NO released in the culture medium of cells cultured on TCP, a-C:H and a-C:H nanotopographies in the presence and absence of BDNF. NO, in fact, has been identified as a paracrine messenger that controls the proliferation and differentiation of neural precursor cells (Cheng *et al.*, 2003; Cappelletti *et al.*, 2003, text references). In our experiment the increase of NO in 300P BDNF+ and BDNF- cultures sustained the induction of hBM-MSCs toward neuronal differentiation. Furthermore, we evaluated the elongation factor (*E*) as the cellular parameter to describe the differences in morphology that occur in cell cytoskeleton architecture and measured the dehydrogenase activity as the cell viability index to avoid signs of stress or toxicity (Martino *et al.*, 2009a). In addition we have analyzed the expression of glial markers. No expression of O4 and GFAP was detected in cells expressing TUJ1 (see Fig. 3). Also measurement of the action potential is a parameter that gives information on the neuronal function.

**Reviewer II:** Why was RPMI used and not a more traditional progenitor cell medium like alpha-MEM?

**Authors:** We isolated, cultured and characterized h-BM-MSCs according to our established protocol (Martino *et al.*, 2009a, text reference)

**Reviewer II:** Why was FCS used only for the initial 24 hours of culture on experimental substrates? If this was to ensure protein deposition for cell adhesion would it not have been better to coat the substrates with fibronectin?

**Authors:** We plated the cells in the presence of FBS for the initial 24h in order to allow canonical cell adhesion and to stabilize cultures according to normal cell plating procedures to avoid phenotypical modification on stem cells.

**Reviewer II:** Why pulse for such a long time? Was incorporation of BrdU not observable after 2-3 hours?

**Authors:** We exposed cells to BrdU for 5h according to the protocol recommended by the manufacturer (BD). Incorporation of BrdU could also be observed after 2-3 hours but we did not test this incubation time.

**Reviewer III:** What is the relative influence of the nanometric height pattern, and that of the differential surface chemistry – introduced by partially covering the glass with a-C:H – on the behavior and differentiation of the cells, and how would you address this?

**Authors:** A key point of our study is the evidence that stem cells are sensitive to grooves with nanometric depth and micrometric width but are influenced by micrometric dimensions. It should be noted, however, that this is a very complex undertaking, which implies the elucidation of signaling network(s) associated with obviously different types of stimulations and possibly affected by crosstalks. At this stages of the work, we showed that the chemical architecture of the substrates influenced protein adsorption, in the order: uniform a-C:H > nanopattern a-C:H (200P  $\cong$  400P  $\cong$  300P) > glass cover slip, TCP, and cell adhesion,

whereas only the 300P grooves micro-geometry was capable to induce the differentiation process.

**Reviewer III:** You link your results strongly to mechanotransductive changes – what is your evidence that the patterning has actually changed the cells mechanical properties – looking at the nuclei they all seem to be more or less round indicating little to no force differential?

**Authors:** Nuclear activation as well as cytoskeleton rearrangements may explain the effect of stem cell interactions with topographies (Ingber, 1993; Charras and Horton, 2002; Dalby, 2005; Wang *et al.*, 2009; Biggs *et al.*, 2010, text references). Depending upon the intensity and direction of such forces, the nucleus could change in terms of eccentricity degree. Even a slight change in nuclear eccentricity degree could be sufficient to generate phenotypical modifications (cell differentiation).

We postulate mechanotransduction as a potential explanation of neural stem cell differentiation because we detected this phenomenon only in 300P a-C:H grooves in the absence of soluble BDNF and in serum-free RPMI. No stem cell differentiation was detected on other substrates under the same culture conditions.